Int. J. Electrochem. Sci., 13 **(2018)** 2164 – 2174, doi: 10.20964/2018.02.65

International Journal of
ELECTROCHEMICAL
SCIENCE
www.electrochemsci.org

Bimetallic Nickel and Copper Supported Pt Catalyst for Ethanol Electro-Oxidation in Alkaline Solution

Lijun Zhang [1,2], *Yuexian Wang*[2], *Zhangna Liu*[2], *Zhaoxiong Yan*[1,*], *Lihong Zhu*[2,*]

[1] Key Laboratory of Optoelectronic Chemical Materials and Devices of Ministry of Education, and Flexible Display Materials and Technology Co-Innovation Centre of Hubei Province, Jianghan University, Wuhan 430056, PR China
[2] Hubei Key Laboratory for Processing and Application of Catalytic Materials, Huanggang Normal University, Huanggang 438000, PR China
[*]E-mail: zhaoxiongyan75@163.com, li_hongzhu@sina.com

Received: 20 October 2017 / *Accepted:* 21 November 2017 / *Published:* 28 December 2017

Bimetallic nickel and copper supported low-content Pt electrocatalyst (Pt/NiCu) was prepared by combining co-electrodeposition of nickel and copper onto a fluorine-doped-tin-oxide (FTO) substrate and chemical reduction of Pt precursor. The performance of the as-prepared catalyst for ethanol electro-oxidation was studied by multi-cyclic voltammetry, current-time curve and electrochemical impedance spectroscopy. The result showed that the molar ratio of Ni/Cu in the electroplating solution had an obvious effect on the activity of the catalysts. Pt/NiCu2 prepared from the solution of 0.02 mol/L $CuSO_4$ + 0.04 mol/L $NiSO_4$ exhibited superior catalytic activity and anti-poisonous tolerance toward ethanol electro-oxidation compared to the solely electrodeposited nickel and copper supported Pt. The excellent performance of Pt/NiCu2 was mainly attributed to the proper molar ratio of Ni/Cu achieving an ideal cooperation of NiCu and Pt, and relatively small charge-transfer resistance.

Keywords: Direct ethanol fuel cells (DEFCs); NiCu nanocomposite; Ethanol electro-oxidation; Electrodeposition

1. INTRODUCTION

The electro-oxidation of small organic molecules, especially ethanol has been a subject of long-term hotspot in the development of portable electronic devices owing to their easy storage and transportation, high energy density, green emission, abundant resource and ambient operation conditions [1-4]. Supported Pt catalysts have been widely explored for ethanol electro-oxidation in acidic and alkaline solutions [5-13]. For example, Pt supported over CeO_2/C [7], SnO*x*/C [8] and MgO/C [9], and alloyed PtM (M=Ru [10]), Sn [11], Cu [12], Ni [13], etc.), and so on, presented

excellent catalytic performance for ethanol electro-oxidation due to the high dispersion of active Pt nanoparticles and/or the synergistic effect of Pt and other transition metals. Moreover, supported or alloyed Pt catalysts also showed enhanced poison-tolerance ability and lower cost compared to the pure Pt catalysts. So far, the design and fabrication of efficient electrocatalysts are still of interest in the research of direct ethanol fuel cells (DEFCs) [14-16].

Nickel has been previously reported as a promoter for ethanol oxidation in DEFCs by activating water molecules and offering active sites for OH adsorption ($H_2O \rightarrow OH_{ads} + H^+ + e$) at lower potentials compared to Pt [17-22]. The generated OH species favor the conversion of the formed CO intermediates into CO_2 via the pathway of $CO_{ads} + OH_{ads} \rightarrow CO_2 + H^+ + e$. The complete oxidation of adsorbed CO into CO_2 can reduce the poison of the electrode. In addition, the nickel (hydr)oxide, especially NiOOH formed during the anodic oxidation of ethanol enhanced the removal of the adsorbed CO-like intermediates which was produced in alcohol electro-oxidation process [23, 24]. Alloyed PtCu catalyst has been mainly investigated for the oxygen reduction reaction due to its superior activity toward the oxygen reduction reaction (ORR) compared to Pt alone [25-27]. Only a small number of investigations have been explored for alcohol oxidation using PtCu catalyst [1, 28]. It is believed that the supports or the alloying elements have an important impact on the electrocatalytic performance of Pt-based catalysts. That is to say, the activity of Pt-based catalysts for ethanol oxidation can be improved by choosing proper supports or alloying elements. Although some investigations associated with PtCu and PtNi catalysts for alcohol oxidation have been studied [28-32], bimetallic Ni and Cu supported Pt for ethanol electro-oxidation has not yet reported in detail. Herein, bimetallic NiCu supported Pt nanoparticles were synthesized for ethanol electro-oxidation, taking advantages of NiCu coating as a support with good conductivity to disperse Pt NPs and cooperative interaction between Ni/Cu and Pt NPs.

2. EXPERIMENTAL

2.1 Preparation

Porous bimetallic NiCu, Cu or Ni coating was electrodeposited onto a FTO conducting glass at a constant potential at room temperature in the corresponding Ni^{2+}/Cu^{2+}, Cu^{2+} or Ni^{2+} solution. The electrodeposited potential was –0.6 V for bimetallic NiCu and Cu; and the electrodeposited time was 600 s and 300 s for bimetallic NiCu and Cu, respectively. The electrodeposited potential was –1.0 V and the time was 600 s for the Ni coating. Pt foil with a large surface area served as a counter electrode, and a saturated calomel electrode (SCE) with salt bridge as a reference electrode. The detailed preparation conditions of the electrode are listed in Table 1. After electrodeposition, the obtained coating was carefully rinsed with distilled water and dried in air. Then 0.05 mL H_2PtCl_4 solution (1 g/100 mL) was added onto the coating, followed by 0.05 mL of the mixed $NaBH_4$ (0.02 mol/L) and NaOH (0.05 mol/L). Finally, the coating was dried at 40 °C in a drying oven, and then carefully washed with distill water. The prepared electrocatalysts were designated as Pt/Ni, Pt/Cu or

Pt/NiCux (x is associated with the concentration of Cu in the mixed electrolyte), respectively (Table 1).

Table 1. The experimental conditions of the electrodes

Samples	Electrolyte compositions	Electrodeposition time / s	Electrodeposition voltage / vs. SCE
Pt/Ni	0.06 mol/L $NiSO_4$	600	-1.0
Pt/NiCu1	0.01 mol/L $CuSO_4$+0.05 mol/L $NiSO_4$	600	-0.6
Pt/NiCu2	0.02 mol/L $CuSO_4$+0.04 mol/L $NiSO_4$	600	-0.6
Pt/NiCu3	0.03 mol/L $CuSO_4$+0.03 mol/L $NiSO_4$	600	-0.6
Pt/Cu	0.06 mol/L $CuSO_4$	300	-0.6

2.2 Characterization

X-ray diffraction (XRD) patterns were examined on a Philips X'Pert powder X-ray diffractometer (Rigaku, Japan) using Cu K_α radiation (λ = 0.15419 nm) at a scan rate (2θ) of 0.05 ° s^{-1}. The morphology and microstructure of the samples were measured on a JEOL JSM-7500 Field emission scanning electron microscopy (FESEM, JEOL, Japan) at a 15 kV accelerating voltage, together with an X-Max 50 energy-dispersive X-ray spectroscopy (EDS, Oxford Instruments, Britain).

2.3 Electrochemical tests

The tests of multi-cyclic voltammetry (CV) and current-time curve were performed on a model LK-2000 microcomputer-based Electroanalysis System (LANLIKE, Tianjin, China). Electrochemical impedance spectroscopy (EIS) measurement was carried out on a CHI660E electrochemical analyzer. The range of the EIS frequency was between 1 Hz and 10 MHz, and the signal amplitude of alternating current (AC) was 5 mV. Zview software was used to analyze the obtained EIS data. The as-prepared electrocatalyst was the working electrode, and Pt foil served as the counter electrode, together with a SCE as the reference electrode. All reagents were analytical grade, and all electrochemical measurements were conducted at room temperature.

3. RESULTS AND DISCUSSION

Figure 1 shows the XRD patterns of Pt/Ni, Pt/Cu and Pt/NiCu obtained from the mixed solutions with different concentrations of Ni^{2+} and Cu^{2+}. The intensities of the XRD patterns for all the samples are weak, mainly due to the amorphous nature and/or small sizes of the nanoparticles. The Pt/Cu catalyst exhibited mixed phases of Pt [33, 34], Cu [35] and CuO/Cu_2O, suggesting the successful

synthesis of Pt/Cu electrocatalyst. Only the characteristic peaks of Pt are observed in the XRD patterns of Pt/Ni, Pt/NiCu1 and Pt/NiCu2. This could be attributed to the alloy of Pt and Ni since platinum is supposed to alloy well with Ni [36].

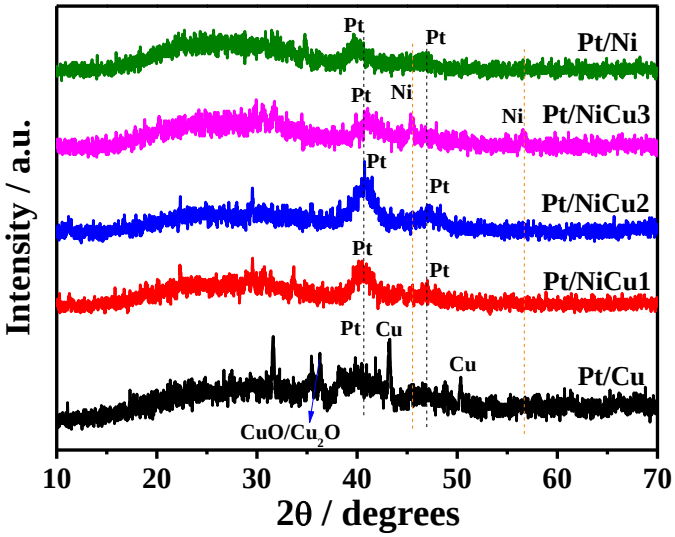

Figure 1. XRD patterns of Pt/Ni, Pt/NiCu1, Pt/NiCu2, Pt/NiCu3 and Pt/Cu.

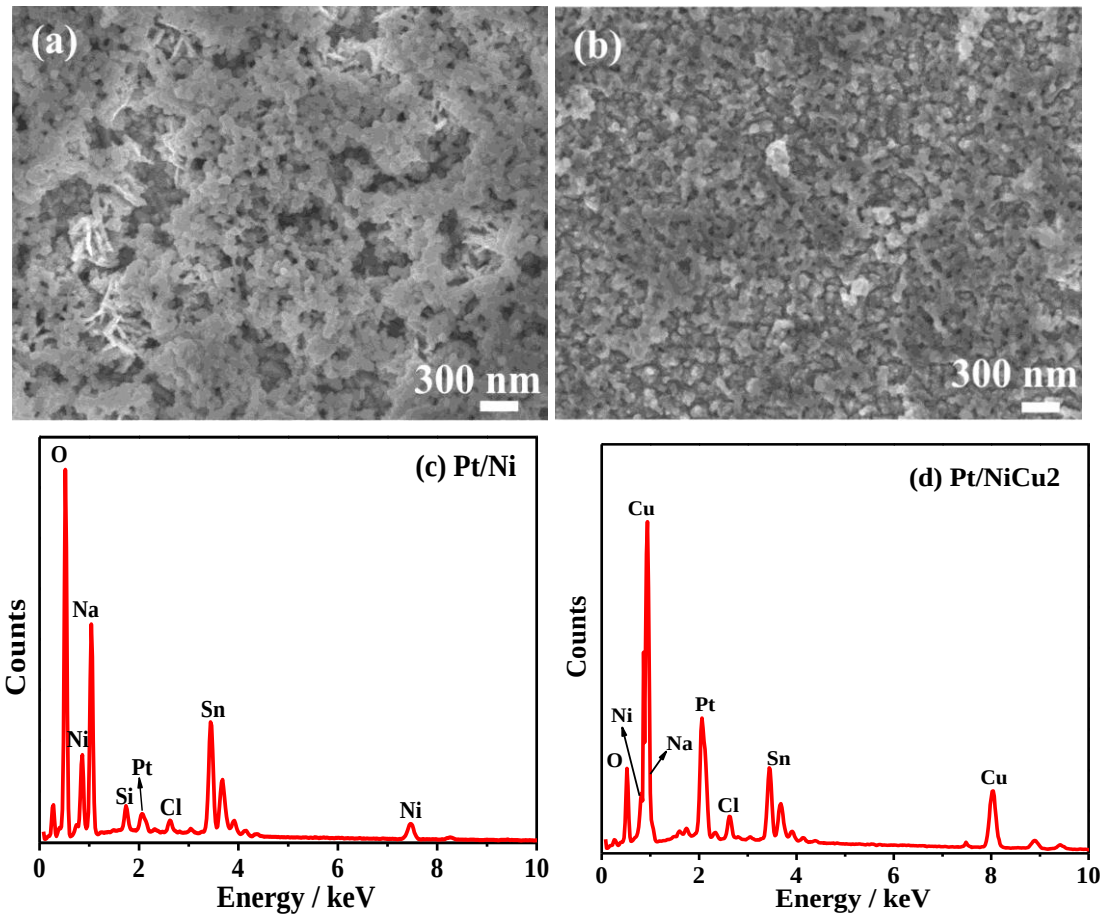

Figure 2. SEM images of Pt/Ni (a) and Pt/NiCu2 (b) catalysts, and EDS of Pt/Ni (c) and Pt/NiCu2 (d) electrodes

Peaks related to nickel/copper hydroxides or oxides were not seen possibly due to their amorphous nature and/or small nanoparticles. No related Cu peaks were clearly observed although the presence of Cu element was confirmed by EDS measurements (see Figure 2d). However, the XRD peaks corresponding to Ni were observed for Pt/NiCu3 [37], indicating the less alloying tendency of Pt and Ni presumably resulted from the retardation of more amount of deposited Cu. The alloying tendency would have an influence on the interaction between Pt and Ni/Cu, and subsequently the activity of the catalyst toward ethanol electro-oxidation.

The morphologies of Pt/Ni and Pt/NiCu2 electrocatalysts are shown in Figure 2a and b. The irregular nanoparticles with sizes at ca. 20–50 nm were deposited evenly on the surface of the FTO substrate. Compared with Pt/Ni, Pt/NiCu2 exhibited much smaller aggregated nanoparticles. Figure 2c and d exhibit the typical EDS spectra of Pt/Ni and Pt/NiCu2 catalysts. Peaks related to O, Ni, Na, Si, Sn, Cl and Pt elements were seen in the spectra of the two samples. Sn and Si signals resulted from the FTO substrate; Na and Cl peaks originated from $NaBH_4$ and H_2PtCl_4 precursors, respectively. O signal was associated with quick oxidation of the deposited Ni/Cu coating. The presence of Ni and Pt confirmed that Ni and Pt were successfully deposited on the FTO substrate. The strong peak of Cu was obviously observed (Figure 2d), suggesting that the successful preparation of bimetallic NiCu nanoparticles.

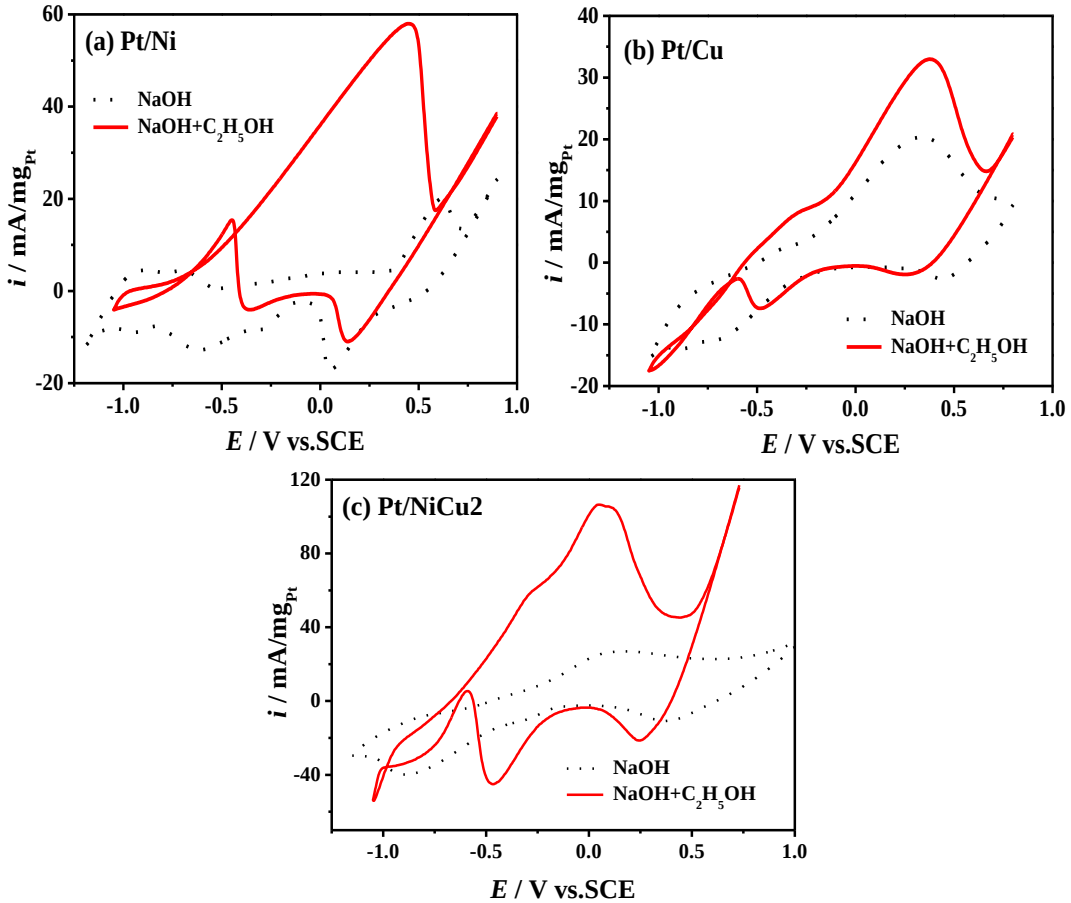

Figure 3. The cyclic voltammograms of Pt/Ni (a), Pt/NiCu2 (b) and Pt/Cu (c) in 1 M NaOH and 1 M NaOH + 1 M C_2H_5OH solutions. Scan rate: 50 mV/s.

Based on the EDS analysis, the loading of Pt was ca. 15% and 18% (wt%) for the Pt/NiCu2 and Pt/Ni, respectively. It indicates that low-content Pt electrocatalysts were successfully prepared. The cyclic voltammograms of Pt/Ni, Pt/NiCu2 and Pt/Cu in 1 M NaOH with and without C_2H_5OH are presented in Figure 3. It can be observed that the CVs in 1 M NaOH + 1 M C_2H_5OH solution displayed different characteristics from those in 1 M NaOH solution. Two well-defined current peaks in the forward and backward scans appeared in 1 M NaOH + 1 M C_2H_5OH solution, featuring the typical electro-oxidation of ethanol. The anodic peak in the forward scan is attributed to the oxidation of freshly chemisorbed ethanol molecules, while the peak in the reverse scan is presumed to associate with the further oxidation of carbonaceous intermediates adsorbed on the electrocatalyst. The activities of the electrocatalysts could be evaluated by the peak current in the forward scan. It can be observed that Pt/NiCu2 showed the largest peak current than Pt/Ni and Pt/Cu, implying that Pt/NiCu2 possessed a superior catalytic performance for ethanol electro-oxidation. Pt/Cu exhibited a relatively poor catalytic activity among the catalysts, presumably due to that copper (hydr)oxides did not participate the oxidation reaction of ethanol. Copper is considered to improve the electrical conductivity and subsequently the electrocatalytic activity of Pt/Ni in ethanol oxidation, which could also be confirmed by the following EIS result.

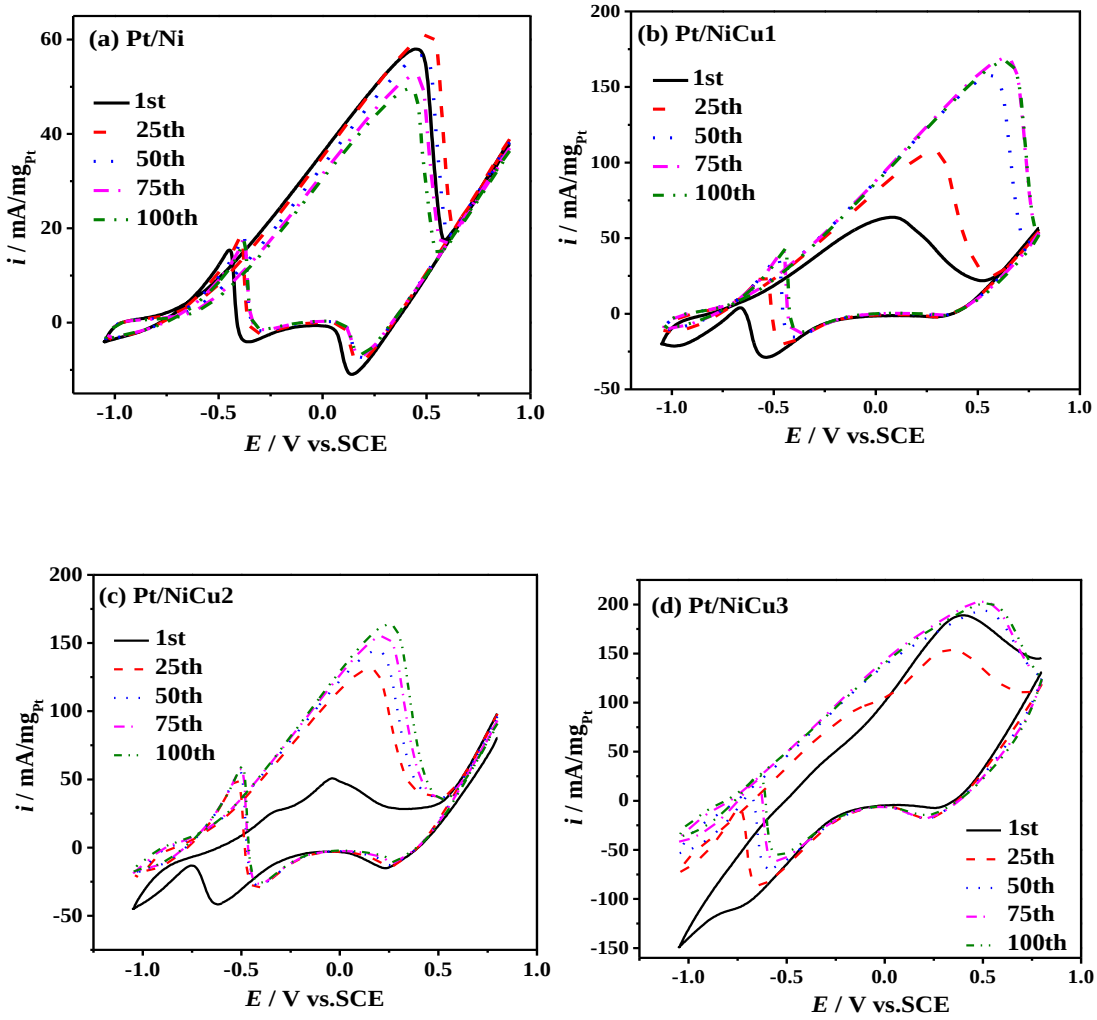

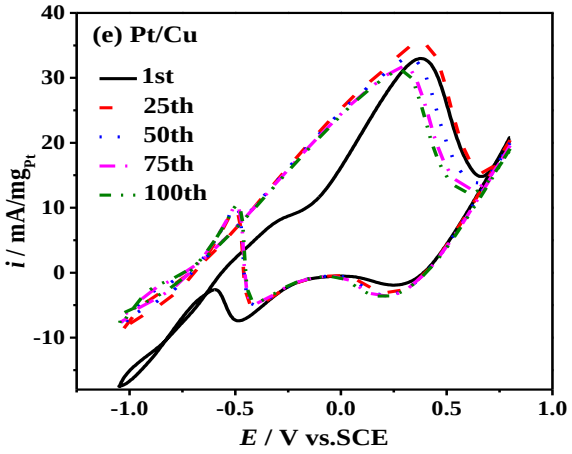

Figure 4. Multiple cyclic voltammograms of Pt/Ni (a), Pt/NiCu1 (b), Pt/NiCu2 (c), Pt/NiCu3 (d) and Pt/Cu (e) in 1 M NaOH + 1 M C_2H_5OH solution. Scan rate: 50 mV/s

Figure 4 shows the multiple CVs of the as-prepared electrocatalysts. An obvious anodic current peak in the forward scan (I_f) and a relatively small current peak in the backward scan (I_b) can be seen for all electrocatalysts. This phenomenon demonstrates the occurence of ethanol electro-oxidation on the electrocatalysts. For Pt/Ni, the peak current in the forward scan increased to the highest value at the 25th cycle, and then decreased with increasing cycle number. For Pt/NiCu1, the peak current in the forward scan rose quickly from the 1st to 50th cycle, and then kept almost unchanged from the 75th to 100th cycle; for Pt/NiCu2, it rose steeply from the 1st to 25th, then increased until the 100th cycle at a very slow rate. This phenomenon indicated that Pt/NiCu2 maintained a relatively high activity toward ethanol electro-oxidation. For Pt/NiCu3, the peak current in the forward scan decreased firstly from the 1st to 25th cycle, then increased to the highest value at the 50th cycle and kept an almost constant value for the rest cycles. For Pt/Cu, the peak current in the forward scan increased firstly and then decreased slightly with increasing the cycle numbers. Closer observation is found that the peak potential in the forward scan shifted to a positive potential with the increase of the cycle number for Pt/NiCu1, Pt/NiCu2 and Pt/NiCu3, while it shifted slightly to a negative potential for Pt/Cu. A higher peak current in the forward scan would result in a more amount of accumulated carbonaceous species on the surface of the electrocatalyst, leading to difficult oxidation of ethanol and higher oxidation potential in the continuous cycle. In addition, Pt/NiCu1, Pt/NiCu2 and Pt/NiCu3 showed larger peak current of ethanol electro-oxidation compared to Pt/Ni and Pt/Cu, mainly due to the electronic structure modification of Pt by Ni and Cu atoms and weakened adsorption energy of carbonaceous species [38, 39]. This reveals that bimetallic NiCu improve the catalytic performance of the sole Ni or Cu supported Pt catalyst. Nickel has been used as a promoter catalyst for ethanol electro-oxidation [20], and its oxyhydroxide (NiOOH) could also provide reactive sites for ethanol electro-oxidation. Incorporation of Cu into Ni could improve the conductivity and porous structure of the catalyst, favoring the transportaion of the charge transfer and the adsorption of carboneous species.

The value of I_f/I_b can be used to evaluate the tolerance of the catalyst to carbonaceous intermediates accumulation. A larger ratio value implies more effective removal of the adsorbed

carbonaceous intermediates during the anodic scan and less accumulation of poisoning residues on the electrode surface; a small I_f/I_b ratio shows the reverse case [40, 41]. Figure 5 presents the dynamic change of I_f/I_b as a function of cycle number. Pt/NiCu1 and Pt/NiCu3 showed a similar tendency of I_f/I_b value with larger I_f/I_b values at the first cycles, and relatively small values in the following cycles. This indicates that the two electrocatalysts were poisoned markedly due to the accumulated intermediates adsorbed on the electrodes in the continuous cyclic voltammograms. The value of I_f/I_b for Pt/NiCu2 increased slightly with increasing the cycle number (inset) although it exhibited the smallest I_f/I_b ratio among the electrocatalysts. By contrast, Pt/Ni and Pt/Cu showed a decay tendency with the increase of the cycle number (inset) as similar to that of Pt/NiCu1 and Pt/NiCu3. This phenomenon reveals that Pt/NiCu2 possessed a stable anti-poison ability during ethanol electro-oxidation.

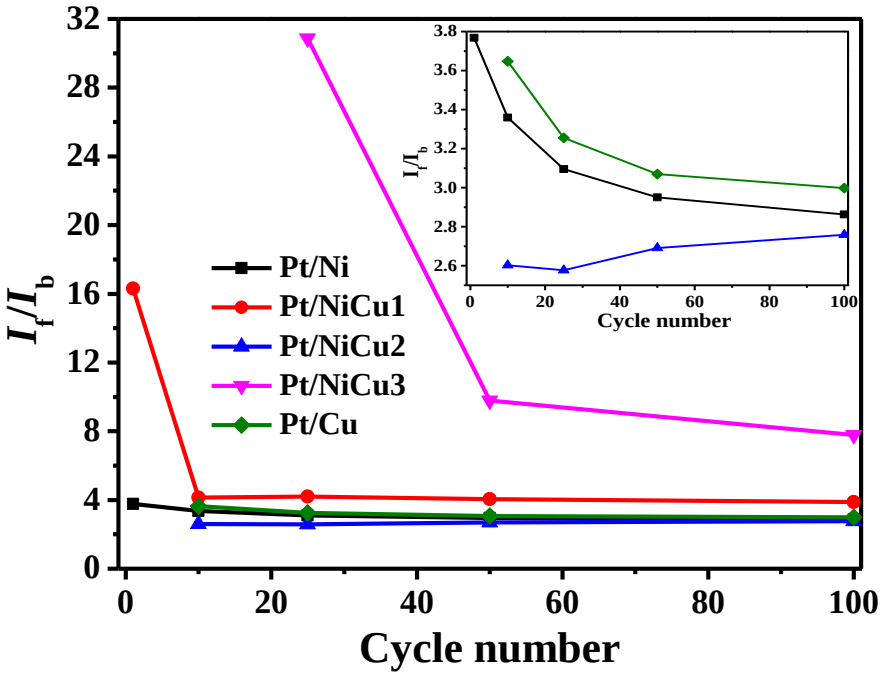

Figure 5. The dynamic change of I_f/I_b as a function of cycle number for Pt/Ni, Pt/NiCu1, Pt/NiCu2, Pt/NiCu3 and Pt/Cu. Inset shows the enlarged image of the change of I_f/I_b with cycle number for Pt/Ni, Pt/NiCu2 and Pt/Cu.

The EIS tests were used to compare the reaction process of ethanol oxidation on the Pt/Ni, Pt/NiCu1, Pt/NiCu2, Pt/NiCu3 and Pt/Cu electrodes. The typical Nyquist plots of the electrocatalysts in 1 M NaOH + 1 M C_2H_5OH solution are presented in Figure 6. The Nyquist plots contained a semicircle in the entire frequency range. The semicircle corresponded to the charge transfer resistance (*R*t) (i.e., ethanol oxidation) in parallel to a constant phase element (CPE). The experimental data were fitted using Zview software and the electrical equivalent circuit was proposed in Figure 6 (inset). The *R*s was the solution resistance, and the CPE was a constant phase element related to the double layer capacitor of the electrode. The *R*s of the Cu-containing catalysts is relatively smaller compared to that

of Pt/Ni mainly due to the enhanced electrical conductivity by Cu. It can be observed that the Pt/NiCu2 electrode showed the smallest Rt value, indicative of the fastest reaction kinetic of ethanol electro-oxidation [42], which might contribute to the higher activity of Pt/NiCu2 electrocatalyst.

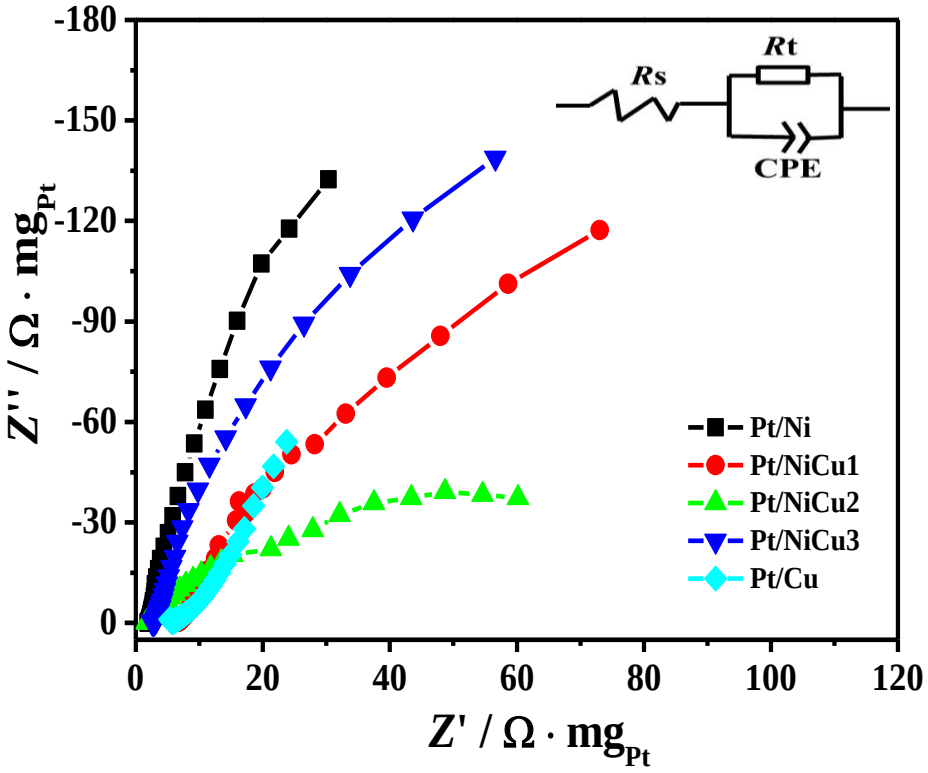

Figure 6. Nyquist plots of Pt/Ni, Pt/NiCu1, Pt/NiCu2, Pt/NiCu3 and Pt/Cu electrodes in 1 M NaOH +1 M C_2H_5OH solution at a potential of 0.1 V.

The performances of Pt/Ni, Pt/NiCu1, Pt/NiCu2, Pt/NiCu3 and Pt/Cu eletrocatalysts for ethanol oxidation were investigated by chronoamperometry in 1 M NaOH + 1 M C_2H_5OH solution at a potential of 0.2 V vs. SCE (Figure 7). An initial current drop in the first 200 s followed by a slower decay was observed in all current-time curves. Pt/NiCu2 showed a higher current and better stability than other studied electrocatalysts. The current of ethanol oxidation over the catalysts increased in the following sequence: Pt/NiCu2 > Pt/NiCu1 > Pt/Ni> Pt/NiCu3> Pt/Cu. It demonstrates the effect of Ni/Cu ratio on the performance of the electrocatalysts. In the bimetallic NiCu supported Pt catalysts, nickel and the produced NiOOH worked as promoter compositions for ethanol electro-oxidation. However, the increasing of NiOOH layer thickness with high ratio of Ni in the catalyst was not preferable to be increased in catalytic oxidation of ethanol since it increased the electrode resistance [43]. The superior performance of Pt/NiCu2 was mainly attributed to an appropriate ratio of Ni/Cu achieving an ideal synergistic effect and relatively smaller *R*t.

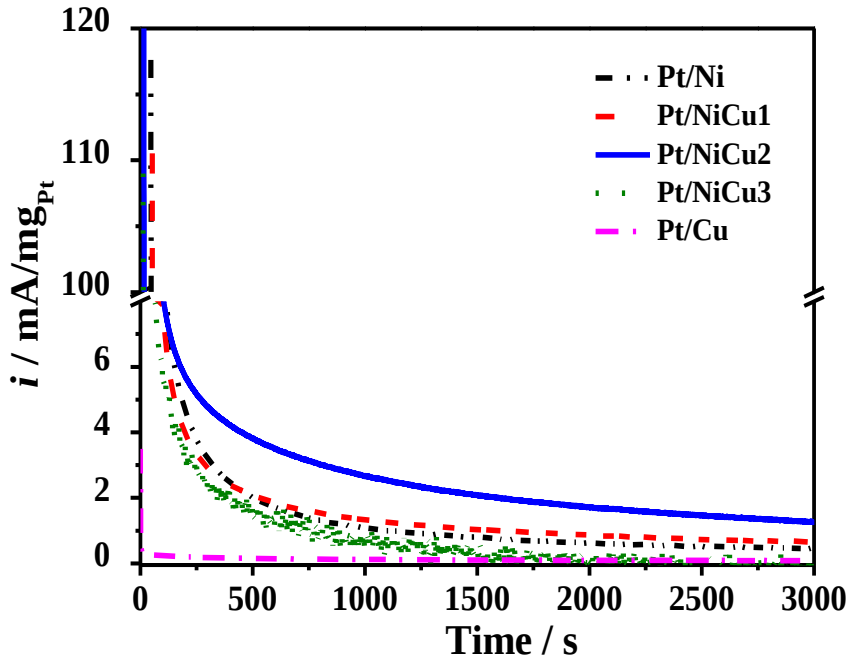

Figure 7. Current-time curves of Pt/Ni, Pt/NiCu1, Pt/NiCu2, Pt/NiCu3 and Pt/Cu. electrodes in 1 M NaOH + 1 M C_2H_5OH solution. Potential: 0. 2 V.

4. CONCLUSION

Bimetallic Ni and Cu supported Pt electrocatalysts were prepared via electrodeposition and $NaBH_4$ reduction processes. The electrochemical investigations showed that the bimetallic NiCu supported Pt electrocatalysts exhibited higher activity toward ethanol oxidation compared with Pt/Ni and Pt/Cu, mainly due to the active species of Ni and electrical conductivity increased by Cu. Pt/NiCu2 exhibited a superior catalytic activity and a long-term stability for ethanol electro-oxidation due to its stable anti-poisoning tolerance and relatively small charge-transfer resistance.

ACKNOWLEDGEMENTS
This work was partially supported by the National Natural Science Foundation of China (21577046 and 21307038), and Wuhan Morning Light plan of Youth Science and technology (2017050304010327).

References

1. R. K. Pandey and V. Lakshminarayanan, *J. Phys. Chem*. C, 13 (2009) 21596
2. Z. Xu, J. Yu and G. Liu, *Electrochem. Commun*., 13 (2011) 1260
3. Y. Miao, L. Ouyang, S. Zhou, L. Xu, Z. Yang, M. Xiao and R. Ouyang, *Biosens. Bioelectron*., 53 (2014) 428
4. Z. Xu, J. Hu, Z. Yan, S. Yang, J. Zhou and W. Lu, *Electrochim. Acta*, 54 (2009) 3548
5. S. K. Meher and G. R. Rao, *J. Phys. Chem*. C, 117 (2013) 4888
6. Z. Xu, L. Rao, H. Song, Z. Yan, L. Zhang and S. Yang, *Chin. J. Catal*., 38 (2017) 305

7. C. Xu and P. Shen, J. Power Sources, 142 (2005) 27
8. L. Jiang, L.Colmenares, Z.Jusys, G. Q. Sun and R.J. Behm, *Electrochim. Acta*, 53 (2007) 377
9. C. Xu, P. Shen, X. Ji, R. Zeng and Y. Liu, *Electrochem. Commun*., 7 (2005) 1305
10. G. A. Camara, R. B. Lima and T. Iwasita, *Electrochem. Commun.*, 6 (2004) 812
11. S. G. Rodríguez, F. Somodi, I. Borbáth, J. L. Margitfalvi, M. A. Peña, J. L. G. Fierro and S. Rojas, *Appl. Catal*. B, 91 (2009) 83
12. M. Ammam and E. B. Easton, *J. Power Sources*, 222 (2013) 79
13. B. Habibi and E. Dadashpour, *Int. J. Hydrogen Energy*, 38 (2013) 5425
14. T. S. Almeida, A. R. V. Wassen, R. B. V. Dover, A. R. Andrade and H. D. Abruňa, *J. Power Sources*, 284 (2015) 623
15. C. Yu, Z. Yan, L. Zhu, J. Wen, H. Wang and Z. Xu, *Electrocatalysis*, 7 (2016) 193
16. X. Lv, Z. Xu, Z. Yan and X. Li, *Electrocatal*., 2 (2011) 82
17. M. A. A. Rahim, R. M. Abdel Hameed and M. W. Khalil, *J. Power Sources*, 135 (2004) 42
18. A. A. El-Shafei, *J. Electroanal. Chem*., 471 (1999) 89
19. E. Antolini, J. R. Salgado and E. R. Gonzalez, *J. Electroanal. Chem*., 580 (2005) 145
20. E. Antolini, J. R. Salgado and E. R. Gonzalez, *J. Power Sources*, 155 (2006) 161
21. Y. Shen, K. Xiao, J. Xi and X. Qiu, *J. Power Sources*, 278 (2015) 235
22. D. Soundararajan, J. H. Park, K. H. Kim and J. M. Ko, *Curr. Appl. Phys*., 12 (2012) 854
23. M. Wang, W. Liu and C. Huang, *Int. J. Hydrog. Energy*, 34 (2009) 2758
24. M. A. A. Rahim, R. M. A. Hameed and M. W. Khalil, *J. Power Sources*, 134 (2004) 160
25. R. Srivastava, P. Mani, N. Hahn and P. Strasser, *Angew. Chem. Int. Edit*., 46 (2007) 8988
26. K. Jayasayee1, J. A. Rob Van Veen, T. G. Manivasagam, S. Celebi, E. J. M. Hensen and F. A. Bruijn, *Appl. Catal*. B, 111-112 (2012) 515
27. M. Oezaslan and P. Strasser, *J. Power Sources*, 196 (2011) 5240
28. T. Page, R. Johnson, J. Hormes, S. Noding and B. Rambabu, *J. Electroanal. Chem*., 485 (2000) 34
29. H. Yang, L. Dai, D. Xu, J. Fang and S. Zou, *Electrochim. Acta*, 55 (2010) 8000
30. E. Taylor, S. Chen, J. Tao, L. Wu, Y. Zhu and J. Chen, *ChemSusChem*, 6 (2013) 1863
31. D. Chen, Y. Zhao, X. Peng, X. Wang, W. Hu, C. Jing, S. Tian and J. Tian, *Electrochim. Acta*, 177 (2015) 86
32. A. B. A. A. Nassr, I. Sinev, M. M. Pohl, W. Grünert and M. Bron, *ACS Catal*., 4 (2014) 2449
33. Y. Mu, H. Liang, J. Hu, L. Jiang and L. Wan, *J. Phys. Chem*. B, 109 (2005) 22212
34. K. W. Park, J. H. Choi, B. K. Kwon, S. A. Lee, Y. E. Sung, H. Y. Ha, S. A. Hong, H. Kim and A. Wieckowski, *J. Phys. Chem*. B, 106 (2002) 1869
35. Z. Xie, C. Xia, M. Zhang, W. Zhu, W. Zhu and H. Wang, *J. Power Sources*, 161 (2006) 1056
36. T. C. Deivaraj, W. Chen and J. Y. Lee, *J. Mater. Chem*., 13 (2003) 2555
37. P. Guan, F. Yan and P. Pei, *J. Power Sources*, 166 (2007) 80
38. Q. Jiang, L. Jiang, S. Wang, J. Qi and G. Sun, *Catal. Commun*., 12 (2010) 67
39. Y. Zhao, X. Yang, J. Tian, F. Wang and L. Zhan, *Int. J. Hydrogen Energy*, 35 (2010) 3249
40. Y. Zhao, L. Zhan, J. Tian, S. Nie and Z. Ning, *Electrochim. Acta*, 56 (2011) 1967
41. L. D. Zhu, T. S. Zhao, J. B. Xu and Z. X. Liang, *J. Power Sources*, 187 (2009) 80
42. R. N. Singh, A. Singh, Anindita and D. Mishra, *Int. J. Hydrogen Energy*, 33 (2008) 6878
43. A. Yousef, R. M. Brooks, M. A. Abdelkareem, J. A. Khamaj, M. M. El-Halwany, N. A. M. Barakat, M. H. EL-Newehy and H. Y. Kim, *ECS Electrochem. Lett*., 4 (2015) F51